CARPATHIAN JOURNAL OF FOOD SCIENCE AND TECHNOLOGY

journal homepage, **https//chimie-biologie.ubm.ro/carpathian_journal/index.html**

RESPONSE OF SECONDARY STRUCTURAL COMPONENTS OF EGG WHITE PROTEINS TO COLD AND THERMAL EXTREMITIES IN WATER/DEUTERIUM OXIDE MIXTURES

İsmail Hakki Tekiner[1,2,3]✉, Anke Knoblauch[3], Alexandru Sover[4], Philipp Häfner[4], Nadja Muschler[3], Marwa Tainsa[5]

[1]Food Engineering Department, Istanbul Sabahattin Zaim University, 34303 Istanbul, Turkey
[2] Nutrition and Dietetics Department, Istanbul Sabahattin Zaim University, 34303 Istanbul, Turkey
[3] Industrial Biotechnology Department, Ansbach University of Applied Sciences, 91510 Ansbach, Germany
[4] Applied Polymer Technology Department, Ansbach University of Applied Sciences, 91510 Ansbach Germany
[5] Department of Agroalimentary, Saad Dahleb University, BP-270 Blida, Algeria
✉ismail.tekiner@izu.edu.tr

https://doi.org/10.34302/crpjfst/2024.16.1.16

Article history:
Received: May 16th, 2023
Accepted: January 12th, 2024

Keywords:
Protein;
Stability;
Denaturation;
Cold;
Thermal.

ABSTRACT

Temperature and water influence proteins' stability and function. This study investigated the response of Amid I secondary structural components (SSC) of egg white proteins to cold (-80 °C) and thermal (100 °C) extremities in water and deuterium oxide (D_2O) mixtures by using FT-IR, DSC, and SEM analyses. Notably, D_2O enabled SSCs exhibit similar profiles at temperature extremities. Latent heat of melting (ΔH_m) raised by 9.5% at 100 °C, while it lowered by 106.8% at -80 °C. Heat capacity (C) increased by 0.9% and 42.2% at 100 and -80 °C, whereas melting temperature (T_m) decreased by 1.7% and 80.5% at 100 and -80 °C. SEM imaging showed flaky structures with different shapes, dimensions, and fissures. Statistical evaluation indicated that there was a strong positive correlation among SSC (*p=0.0001*), ΔH_m (*p=0.00008*), and C (*p=0.00001*) changes, except for T_m values (*p*=.558182). Overall, D_2O contributed to protein stability at 100 and -80 °C by controlling the unfolding process, possibly by an enthalpy-dependent mechanism. Therefore, it can be used as a reference solvent to establish kinetic models with/without enzymatic, physical, or chemical approaches for improved protein stability.

1. Introduction

The process optimization is based on scale-up rules and optimization paths assuming (near) equilibrium. However, the foods do not always rely on this assumption of (near) equilibrium (Burbidge and le Révérend, 2016). Adapting proteins to extreme physical conditions requires complicated and diverse intermolecular interaction alterations (Zhang et al., 2021). Many extrinsic and intrinsic stressors influence their stability, and to our knowledge, no current solutions have satisfied this requirement satisfactorily (Yousefi and Abbasi, 2022). Protein stability determines whether a protein stays in its native folded conformation or a denatured state. Its estimation plays an essential role in food design and the fate of food processing by opening the way to improved food products (Goldenzweig and Fleishman, 2018). Proteins' folded and unfolded states are related to protein stability, and α-helices and β-sheets are essential determinants of folded protein structure (Baronio and Barth, 2020). Protein unfolding caused by heating is referred to as "thermal denaturation," whereas it is so-called "cold denaturation" in the case of cooling. Protein goes from a naturally folded state to a random coil in an aqueous solution with rising temperature. In contrast, cold denaturation is transitioning to a denatured state with decreasing temperature (Ballauff, 2022). Heat denaturation is typically an everyday experience because it can degrade many systems. However, lowering the temperature, "cold" generally slows down processes to eventually stabilize a system (Sanfelice and Temussi, 2016). Moderating proteins' stability or instability at temperature fluctuations remains speculative, at least to some extent (Weiss et al., 2018).

Water is a complex substance with various unusual properties due to its ability to form hydrogen bonds. Therefore, it plays an important role in governing proteins' structure, stability, dynamics, and function (Sen et al., 2009). Deuterium oxide (D_2O) is an isotopic form of regular water with relatively higher density (1.107 g/mL), melting (3.82 °C), and boiling (101.4 °C) temperatures. It forms hydrogen bonds stronger than in typical aqueous environments, resulting in stronger interactions among structural proteins and sticking them with one another together (Schnauß et al., 2021). Therefore, it can be used for isotopic labeling of salt micelles, oleosomes, carbohydrates, and deuterated alcoholic beverages and the stability of globular proteins, cells, and tissues (Pica and Graziano, 2017). In addition, several works investigated its impact on the peptization of some amino acids such as Phe, His, Pro, Cys, and Met (Fulczyk et al., 2019), and lipid oxidation of corn oil and linoleic acid (Oh et al., 2017; Lee et al., 2018). However, to our knowledge, no study has been conducted to examine its influence on the proteins of food origin. Adopting egg and egg-derived products to thermal extremities and higher water activity improves their stability during food design, processing, and storage. This study investigated the response of Amid I secondary structural components (SSC) (antiparallel β-sheet/aggregated strands, 3_{10} helice, α-helix, unordered, β-sheet, and aggregated strands)) of egg white proteins to cold (-80 °C) and thermal (100 °C) extremities in water and deuterium oxide (D_2O) mixtures by using FT-IR, DSC, and SEM analyses.

2. Materials and methods

2.1. Materials

D_2O (99.9 atom % D) was purchased from Sigma Aldrich (Catalogue no: 151882-250G, Darmstadt, Germany), and fresh hen eggs from a market in Ansbach, Germany.

2.2. Methods

2.2.1. Sample preparation

The fresh hen egg was broken, and its white (EW) was separated in a 50 mL glass beaker by removing its chalazae. Two sampling series (T and C) were prepared separately. Each series was comprised of seven glass vials (T0, T1, T2, T3, T4, T5, T6; and C0, C1, C2, C3, C4, C5, C6) for thermal (T) and cold (C) treatments. The vials T0 and C0 contained 2 mL of fresh EW only, and T1 and C1 included 2 mL of fresh EW and distillate water (dW). In comparison, the remaining vials of both series had 2 mL of fresh EW and different concentrations of D_2O ranging over 20%, 40%, 60%, 80%, and 100% (v/v) (Table 1). The vials were closed with a cap and vortexed for 2 min.

Table 1. Composition of EW blends with/without dW and D_2O

Sample	**T0/C0**	**T1/C1**	**T2/C2**	**T3/C3**	**T4/C4**	**T5/C5**	**T6/C6**
V_{EW} (mL)	2	2	2	2	2	2	2
V_{dW} (mL)	0	3	2.4	1.8	1.2	0.6	0
V_{D2O} (mL)	0	0	0.6	1.2	1.8	2.4	3
V_{Total} (mL)	2	5	5	5	5	5	5

2.2.2. Thermal (T) and cold (C) treatments

After overnight storage, the samples were kept in room condition. The T-series was heated up to 100 °C in a shaking-water bath (Julabo SW22, Seelbach, Germany) for 40 min, followed by storing at + 4 °C for a few min to stop the thermal denaturation process. Similarly, the C-series was cooled to -80 °C in a cryogenic freezer (Smart-Cryo SWLF, Aachen, Germany) for 40 min and kept in a water bath at room temperature few min to stop the cold denaturation process (Rossi and Schiraldi, 1992).

2.2.3. FT-IR and curve fitting analyses

After thermal and cold treatments, the samples were freeze-dried using Epsilon 1-4 LSC plus freeze-dryer (Martin Christ, Osterode am Harz, Germany). They were initially subjected to freezing at -40 °C. Subsequently, the shelf temperature was set at −40 °C, and drying ended at 20 °C under a vacuum of 0.150 mbar for 72 h. After freeze-drying (FD) is over, the samples were kept in a desiccator over phosphorpentoxid (P_2O_5) (Merck 1.00540.1000, Darmstadt, Germany) at room temperature for several days to completely dry (Zhao et al., 2020). After the FD, about 100-µg freeze-dried sample was subjected to FT-IR analysis (Thermo Scientific Nicolet iS50 FT-IR, Dreieich, Germany). All FT-IR spectra were recorded at room temperature between 4000 and 650 cm^{-1} after 32 scans with a spectral resolution of 4 cm^{-1}. The curve fitting for the Amide I band was conducted to quantitatively investigate the changes in secondary structural components. The second derivative spectrum determined the number of bands: 1675 to 1695 cm^{-1} for antiparallel β-sheet/aggregated strands, 1660 to 1670 cm^{-1} for 3_{10} helice, 1648 to 1660 cm^{-1} for α-helix, 1640 to 1648 cm^{-1} for β-sheet, and 1610 to 1628 cm^{-1} for aggregated strands. The relative amounts of secondary structural components based on the modeled peak areas were calculated according to the report generated by the Thermo Fisher Scientific OMICS software (Jackson and Mantsch, 1995; Kong and Yu, 2007).

2.2.4. Thermal (DSC) analysis

The samples were analyzed for determining the changes in the latent heat of melting (ΔH_m, J/g), melting temperature (T_m, °C), and heat capacity (C, J/gK) using Mettler Toledo Differential Scanning Calorimetry (DSC) (Greifensee, Switzerland). An amount of 5 to 10 mg of the treated sample was measured. The temperature range was selected as 20 °C to 100 °C for the T-series, whereas it was set as 20 °C to -80 °C for the C-series with a scan rate of 5 °C/min. The Mettler Toledo STARe 17 software was used for thermal analysis (Mettler Toledo, 2022).

2.2.5. Scanning electron microscopy (SEM) analysis

The microstructure of the samples was studied using Tescan Clara GMU SEM (Bruno, Czech Republic). To improve conductivity and image contrast, all the samples were initially subjected to surface treatment at 0.30 mbar/3 min for cleaning, etching, and activating the samples by Diener Tetra 30-LF-PC (Nagold, Germany). Subsequently, they were coated with a layer of Pt/Pd in an argon atmosphere (30 mA, 0.1 mbar, 30 s) to sputter conducting layers to prevent charging effects by Cressington 108 Auto Sputter Coater (Watford, UK). The acceleration voltage used in SEM was 5 keV, the beam current was 5×10^{-9} mA, and the working distance was 6 mm. The microstructure of the samples was viewed and photographed at a magnification of 2.23 kx (Liu et al., 2015).

2.2.6. Statistical evaluation

The strength of association between Amid I secondary structural components, ΔH_m, T_m, and C values of T- and C-treated samples were tested with the Pearson correlation coefficient method using SPSS statistical package program at *$p<0.01$*.

3.Results and discussions

This study evaluated the response of Amide I secondary structural components of fresh EW proteins to 100 °C and -80 °C in different concentrations of dW and D_2O by FT-IR, DSC, and SEM analyses. Overall, D_2O contributed to the protein stability of EW at 100 °C and -80 °C by indirectly controlling the unfolding process.

3.1. Results of FT-IR and curve fitting analyses

The curve fitting analysis for the Amide I band was investigated for quantitative estimation of antiparallel β-sheet/aggregated strands, 3_{10} helice, α-helix, unordered, and β-sheet, and aggregated strands in T (100℃) and C (-80℃) series (Table 2, Figure 1).

3.1.1. Response of fresh EW to temperature extremities

Abrosimova et al. (2016) found the frequencies of α-helix, β-sheet, and unordered strands in the raw EW to be 33%, 38%, and 12%, respectively, whereas they were 4%, 54%, and 6% in the boiled EW. Luo et al. (2022) reported that heating makes the protein structure disordered, i.e., a decrease in α-helix content increase in β-sheet content. In our study, the reference sample T0 contained only 2 ml of fresh EW. After the heat treatment, the major strand in T0 was α-helix (98.4%), followed by antiparallel β-sheet/aggregated strands (0.6%), 3_{10} helice (0.3%), β-sheet and aggregated strands (0.2%), and unordered (0.1%), respectively. Our SSC results of T0 were different from Abrosimova et al. (2016) and Luo et al. (2022). Freezing is generally used to maintain quality and extend the shelf life of foods. Lee et al. (2022) determined that freezing at -18 °C caused the denaturation of proteins, altered the secondary structure, and increase in β-sheet content and decrease in α-helix at -60.15 °C, in line with Hu and Xie (2021) and Li et al. (2021). However, Sun et al. (2016) and Hu et al. (2021) oppositely reported a decrease in β-sheet content. In our study, the major SSCs in the reference sample C0 including 2 ml of fresh EG only -80 °C were β–sheet/aggregated (24.5%) and unordered strands (16.9%), indicating the deterioration of some functional and sensorial qualities of EW before processing. Our SSC results of C0 matched with Hu and Xie (2021) and Li et al. (2021).

3.1.2. Response of fresh EW to temperature extremities in dW

Regular water can stabilize proteins, particularly globular ones, through hydrophilic and hydrophobic interactions. The interaction of proteins with water makes the FT-IR analysis of SSCs difficult. However, its evaporation may also destabilize the helical structure of a protein, i.e., an increase in β-sheet strands and α-helix decrease (Abrosimova et al., 2016). In addition, higher water activity (a_w) makes egg and egg-derived products perishable and highly susceptible to physicochemical changes (Kocetkovs et al., 2022). In our study, sample T1 included 2 ml of fresh EW in 3 ml of dW only. The common strand in T1 was the antiparallel β-sheet/aggregated (20.5%), followed by unordered (18.4%) and α-helix (17.1%) strands. Our sample C1 contained only 2 ml of fresh EW in 3 ml of dW. For C1, the α-helix (30.1%) was the dominant strand, followed by antiparallel β-sheet/aggregated strands (25.6%) and 3_{10} helice (15.7%) strands. Overall, dW could stabilize the EW proteins at -80℃ compared to the sample T1 at 100℃. Therefore, our findings provided data about the response of the SSCs of EW proteins to 100℃ and -80℃ in the solution of regular water (dW).

3.1.3. Response of fresh EW to temperature extremities in dW and D_2O

D_2O can stick proteins with one another together by forming hydrogen bonds strong-er than in solutions of regular water (Schnauß et al., 2021). It might weaken the strength of the van der Waals attractions between EW proteins and water molecules, leading to the protection of hydrogen bonds and electrostatic interactions responsible for the stability of proteins (Luo et al., 2022). An average equivalent of 7-25% D_2O can prevent protein denaturation in vaccines, and the presence of 95% D_2O is equivalent to a 4-5 °C reduction in storage temperature relative to regular water (Sen et al., 2009). The reference samples T2 to T5 and C2 to C5 contained 2 mL of fresh EW and different concentrations of D_2O (from 20%, 40%, 60%, and 80% in ascending order), and T6 and C6 included 100% of D_2O as the diluent. The primary strand in T2, T3, T4, and T5 samples was α-helix (29.4 ± 7.1%), followed by antiparallel β-sheet/aggregated (21.3 ± 3.7%). Similarly, the frequencies of the common SSCs in C2, C3, C4, and C5 were found to be α-helix (32.3 ± 1.7%) and antiparallel β-sheet/aggregated (24.5 ± 1.2%) strands, respectively.

Table 2. FT-IR spectra and estimated area changes of Amid I secondary structural components

Sample no	λ_{peak} (cm^{-1}) *	$\sum A_{peak}$ (cm^2)	Estimated area of strands (%)						
			Antiparallel β-sheet/ aggregated strands	**3_{10} helice**	**α-helix**	**Unordered**	**β-sheet**	**Aggregated strands**	**Indefinite**
T0 (Reference)	1629.15	1.01353	0.6	0.3	98.4	0.1	0.2	0.2	0.2
C0 (Reference)	1634.54	0.02249	24.5	15.2	14.7	16.9	9.3	10.2	9.2
T1 (100% dW)	1625.96	0.02380	20.5	15.9	17.1	18.4	7.9	9.4	10.8
C1 (100% dW)	1635.42	0.02407	25.6	15.7	30.1	3.7	9.1	6.6	9.3
T2 (20% D_2O)	1625.35	0.01307	25.2	10.7	20.4	6.8	6.0	14.1	16.8
C2 (20% D_2O)	1633.47	0.03159	23.5	14.7	30.7	4.3	10.1	8.0	8.6
T3 (40% D_2O)	1624.11	0.01932	23.7	10.7	27.2	4.1	6.3	10.2	17.8
C3 (40% D_2O)	1633.85	0.03369	25.7	15.7	34.8	4.1	8.9	1.6	9.1
T4 (60% D_2O)	1624.10	0.03294	18.2	7.7	35.4	3.3	10.2	11.4	13.8
C4 (60% D_2O)	1633.98	0.02783	23.5	14.4	31.6	3.8	10.1	8.2	8.4
T5 (80% D_2O)	1623.80	0.03113	18.1	14.9	34.7	0	9.8	10.2	12.4
C5 (80% D_2O)	1633.95	0.02125	25.4	8.5	32.0	4.8	10.1	10.7	8.6
T6 (100% D_2O)	1622.00	0.02233	18.0	17.2	37.8	0	9.2	6.9	10.9
C6 (100% D_2O)	1633.35	0.02809	23.3	14.4	33.4	3.8	8.6	8.3	8.2

*Amide I spectra: 1700 to 1600 cm^{-1}

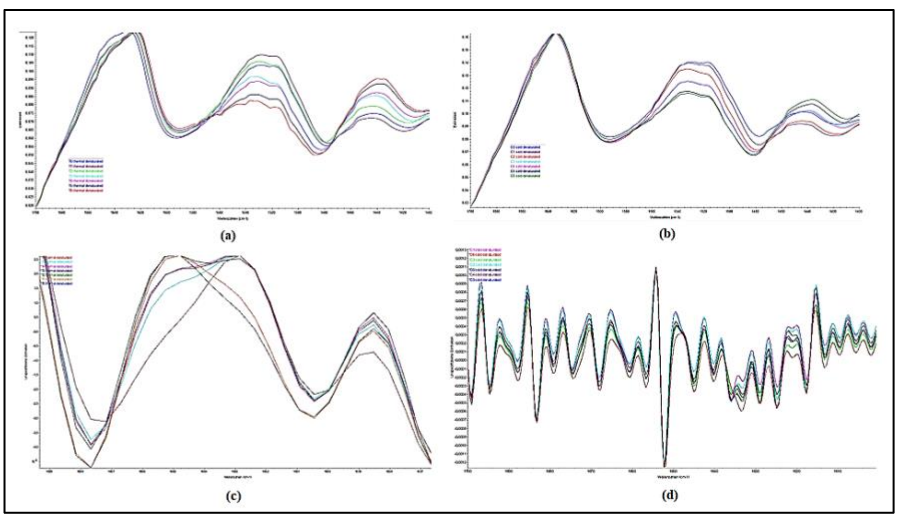

Figure 1. FT-IR spectra and second derivative of Amid I band of T and C series: (a) FT-IR spectra of T-series, (b) FT-IR spectra of C-series, (c) second derivative spectra of T-series, and (d) second derivative spectra of C-series

Besides, for the samples T6 and C6 including 100% D_2O as the diluent, the contents of the α-helix strand were detected to be 37.8% and 33.4%. Denaturation relates to the number of α-helical strands (Van Der Plancken et al., 2006). D_2O could tolerate the temperature extremities by making the protein more compact and less flexible than in dW through the hydrophobicity effect (Clark et al., 2019). For instance, hen egg lysozyme was more stable in D_2O than H_2O (Pica and Graziano, 2017). Our findings matched with Van Der Plancken et al. (2006), Sen et al. (2009), Abrosimova et al. (2016), and Pica and Graziano (2017), respectively. Accordingly, D_2O could positively moderate the transformation of α-helix strands to other unordered strands under temperature extremities. Our study, therefore, contributed to the knowledge gap by providing data over D_2O on the EW proteins for the food area.

3.2. Results of thermal (DSC) analysis

Our DSC thermograms indicated that the ΔH_m, T_m, and C values for T0, T1, and T2 to T6 were found as 118.6 J/g, 69.8 °C and 206.4 J/gK, 131.7 J/g, 68.1 °C and 220.1 J/gK, and 129.9 ± 7.0 J/g, 68.6 ± 1.3 °C, and 208.1 ± 6.0 J/gK, respectively, whereas those of C0, C1, and C2 to C6 were measured as -60.1 J/g, 17.1 °C and 70.0 J/gK, -133.4 J/g, 8.9 °C and 106.6 J/°C, and -124.3 ± 63.9 J/g, 3.3 ± 4.0 °C and 99.5 ± 11.1 J/gK, respectively. Overall, D_2O raised ΔH_m and C by 9.5% and 0.9% at 100 °C and 106.8% and 42.2% at -80 °C, whereas T_m decreased by - 1.7% at 100 °C and -80.5% at -80 °C (Table 3, Figure 2).

3.2.1. Results of ΔH_m measurement

The behavioral characteristics of the heat- and cold-denatured proteins remain a theoretical issue (Oshima et al., 2009). Thermal denaturation is associated with increased entropy for protein unfolding, whereas cold denaturation is driven enthalpically (Lee et al., 2022). A decrease in denaturation enthalpy indicates a partial loss of protein structure during heating (Van Der Plancken et al., 2006). For many proteins, denaturation is a two-state transition, relating T_m to the transition enthalpy, and EW is an example of a heat-setting thermo-irreversible gel (Ballauff, 2022). From this perspective, our study provided data for determining how cold-denatured EW would differ from heat-denatured.

In the literature, the denaturation enthalpy of fresh EW was reported to be 20.6 J/g (Ferreira et al., 1997) and 15.3 J/g at -19.0℃ (Wootton et al., 1981). In our study, ΔH_m values of T- and C-series with different concentrations of D_2O (i.e., 20%, 40%, 60%, 80%, and 100%) were measured as 129.9 ± 7.0 J/g (max 139.5 J/g for T2 with 20% D_2O), and -124.3 ± 63.9 J/g (lowest -229.7 J/g for C6 with 100% D_2O), respectively, whereas they were 118.6 J/g for T0 and -60.1 J/g for C0 (EW only), and 131.7 J/g for T1 -133.4 J/g for C1 (EW and dW only). Our findings of ΔH_m at 100 °C and -80 °C exhibited specific characteristics and various changes compared to fresh EW and dW, including samples. In our case, D_2O could tolerate energy fluctuations, increasing the heat-absorbing capacity for EW blends.

Table 3. Results of thermal (DSC) analysis: ΔH_m (J/g), T_m (°C) and C (J/gK)

Parameter / Sample no	**T0**	**T1**	**T2**	**T3**	**T4**	**T5**	**T6**
Latent heat of melting (ΔH_m, J/g)	118.6	131.7	139.5	122.4	134.2	125.0	128.3
Peak (T_m, °C)	69.8	68.1	66.8	68.9	70.4	69.0	68.0
C (J/gK)	206.4	220.1	208.3	198.8	212.7	206.9	213.9
Parameter / Sample no	C0	C1	C2	C3	C4	C5	C6
Latent heat of melting (ΔH_m, J/g)	-60.1	-133.4	-126.5	-96.4	-109.7	-59.3	-229.7
Peak (T_m, °C)	17.1	8.9	5.1	1.1	0.8	9.6	0.1
C (J/gK)	70.0	106.6	108.7	86.3	107.5	106.6	88.5

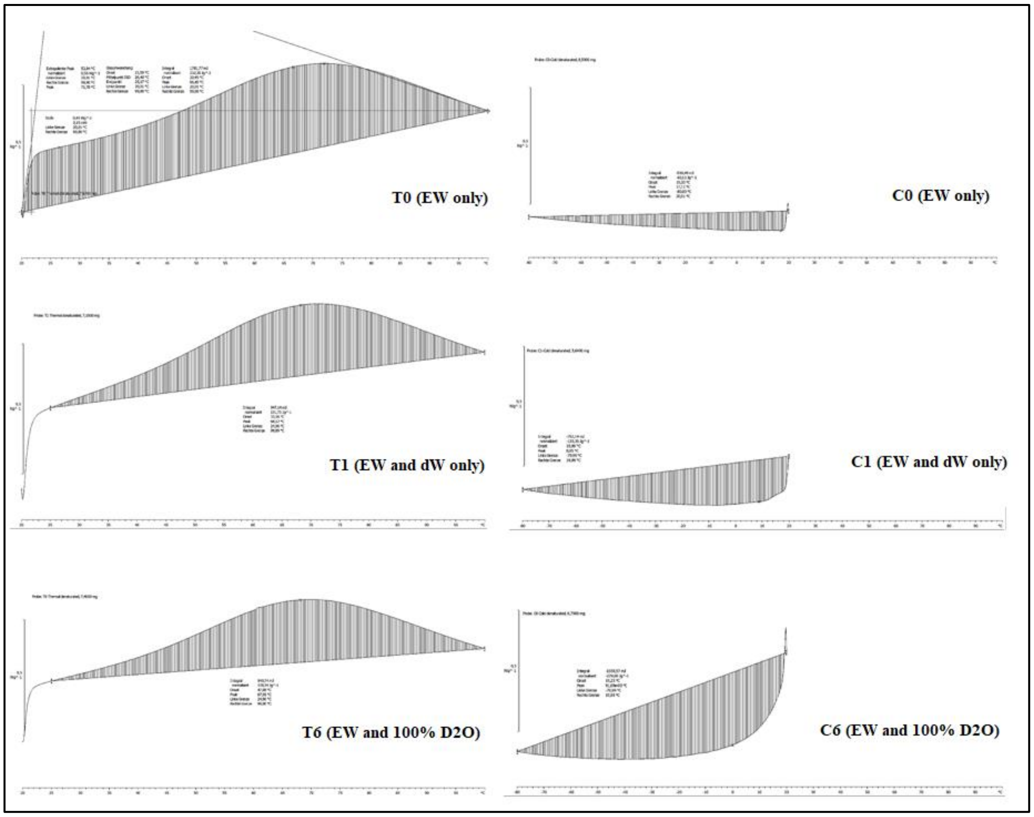

Figure 2. DSC thermograms of T- and C-series

To understand this intriguing phenomenon, i.e., heat and cold denaturation, a two-state model of water structure, as proposed by Tsai et al. (2002), can be considered to explain the role of the physicochemical properties of D_2O with ice dominating at -80℃ and liquid state at 100 ℃, to figure out which folding ↔unfolding steps are entropy-driven, and which are enthalpy driven, possibly an enthalpy-dependent process in our study. Overall, our findings point out that D_2O has significant potential to be utilized for protein stability compared to enzymatic, physical, or chemical approaches.

3.2.2. Results of T_m measurement

A common issue in protein stability is the change in the T_m of a protein in the aqueous phase. Denaturing a protein's native structure is so-called melting. However, some protein SSCs can remain after denaturing above T_m and do not necessarily melt at typical processing temperatures (Bier et al., 2014). In the literature, some works observed the different peaks of T_m of EW as 72℃ and 86 °C (Wootton et al., 1981), 50 °C and 65 °C (Der Plancken et al., 2006), and 60 °C (Ferreira et al., 1997). In our study, the average T_m values of T- and C-series with different concentrations of D_2O (i.e., 20%, 40%, 60%, 80%, and 100%) were determined to be 68.6 ± 1.3 °C (max 70.4 °C for T4 with 60% D_2O) and 3.3 ± 4.0 °C (max 9.6 °C for C5 with 80% D_2O), respectively. At the same time, they were 69.8 °C and 17.1 °C for T0 and C0 (EW only) and 68.1 °C and 8.9 °C for T1 and C1 (EW and dW only), respectively. Our findings showed that, for D_2O containing T- and C-series samples, the T_m values changed by -1.7% at 100 °C and -80.5% at -80 °C. Denaturation is a two-state transition, relating T_m to the transition enthalpy (Ballauff, 2022). In our study, D_2O might absorb more heat without relatively changing T_m through a temperature-independent process. On the other hand, in cold denaturation, the reduction of T_m by -80.5% might enable the EW proteins to remain after denaturing.

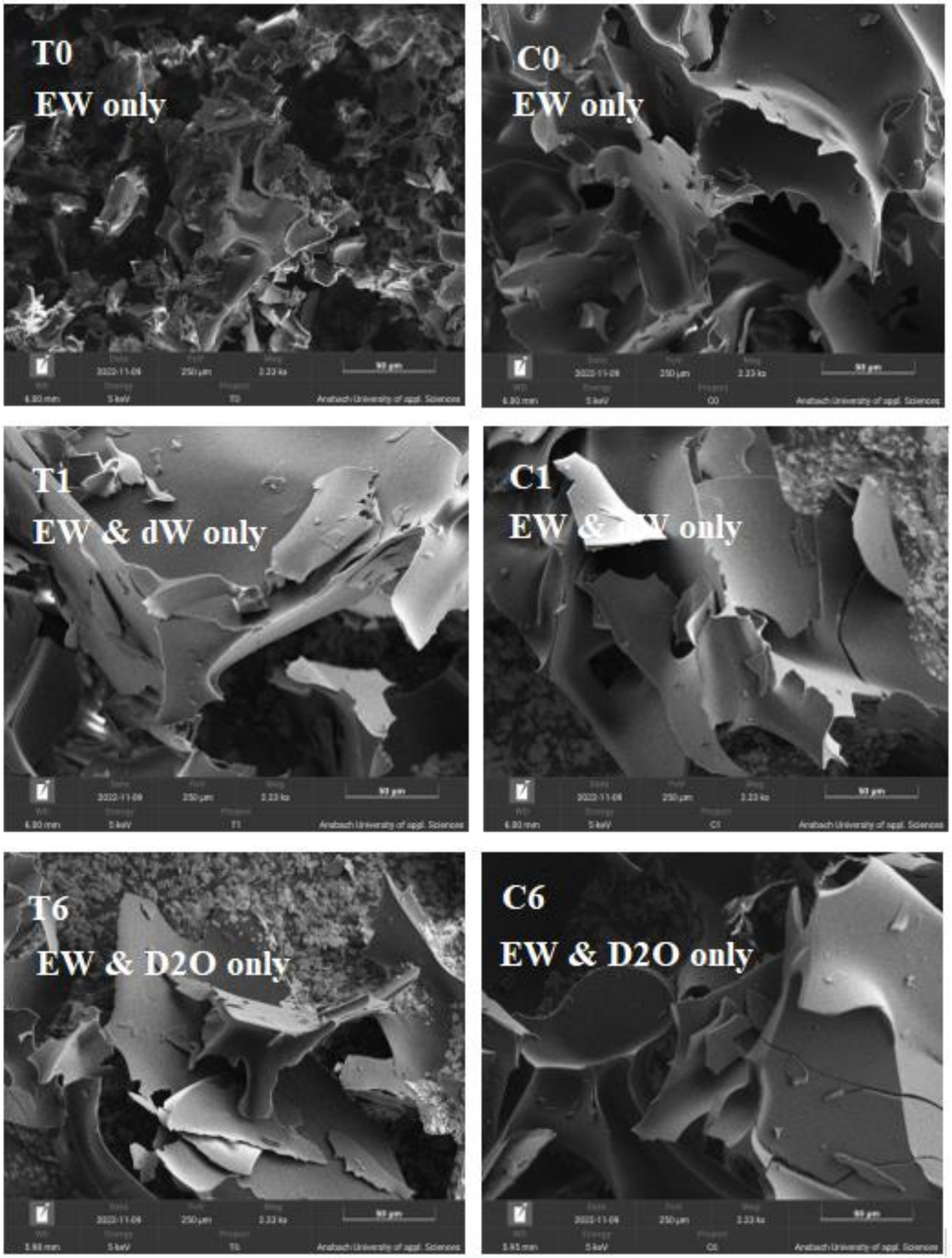

Figure 3. SEM images of T-and C-series (magnification 2.23 kx)

3.2.3. Results of C measurement

Heat capacity (C) is one of the significant thermophysical properties of foods over a broad range of T and a_w required for evaluating, designing, and modeling heat transfer processes. In the literature, some studies reported the C value of EW as 2.6 to 3.7 J/gK at temperatures ranging from 0 to 38℃ and water concentrations from 51.8 to 88.2% (Coimbra et al., 2006) and 2600 to 3.7 J/gK (Lee et al., 2016). An increase in C makes a significant contribution to the total unfolding enthalpy. The increment of C is temperature-independent between 20 to 80℃, and C of native and denatured states changes in parallel with an increase in T, proceeding with heat absorption and, consequently, with increases in enthalpy and entropy. However, in the case of cooling, it proceeds with heat release and, thereby, with enthalpy and entropy reductions (Privalov, 1990). In our study, D_2O raised C by 0.9% at 100 °C (ave. 208.1 ± 6.0 J/gK) and 42.2% at -80 °C (ave. 99.5 ± 11.1 J/gK), whereas it was 206.4 J/gK and 70.0 J/gK for T0 and C0 (EW only), and 220.1 J/gK and 106.6 J/gK for T1 and C1 (EW and dW only), respectively. Our findings revealed that D_2O might act as an energy-absorbing buffer at 100 ℃ and an indirect controller of unfolding enthalpy and entropy at -80 °C.

3.3. Results of SEM analysis

Our study captured the SEM images with a magnification of 2.23 kx of the T and C series (Figure 3).

Ogawa et al. (2003) demonstrated that heated-dried EW comprised small gel structural units that formed a dense and heterogeneous network, suggesting the suppression of protein aggregation. In contrast, nonheated-dried EW comprised large protein particles that formed coarse and random networks. Preethi et al. (2021) detected that conductive hydro-dried EW had a flaky structure, while spray-dried and freeze-dried flakes exhibited spherical and porous structures. Our SEM images exhibited flaky structures for both treatment groups with different shapes, dimensions, and fissures, which can indicate the thermal behavior of proteins related to the influence of D_2O on protein stability.

3.4. Results of statistical evaluation

Pearson correlation coefficient calculator was used to measure the strength of a linear association between the T and C treatment series. All analyses were performed using SPSS statistical package program. A *p*-value less than 0.01 was considered statistically significant. The statistical evaluation indicated that there was a strong positive correlation among SSCs ($p=0.0001$), ΔHm ($p=0.00008$), and C ($p=0.00001$) changes at temperature extremities, except for Tm values ($p=0.558182$).

4. Conclusions

Understanding the stability of proteins is of great interest among food science and technology researchers, resulting in an insight into the physicochemical principles that govern the changes and reactions in food processing. The results presented in this study have significant implications for the behavior of amino acids in complex food matrices (EW) under temperature extremities: (a) D_2O influences protein stability to temperature extremities, (b) D_2O indirectly controls unfolding process, (c) D_2O possibly acts through enthalpy-dependent process, and (d) D_2O can be used to establish kinetic models for stable protein-rich foods, respectively. Therefore, it can be used as a reference solvent with its unique properties to establish kinetic models for biomacromolecules with prolonged stability, as an alternative and/or complementary substance to other methods, including enzymatic, physical, or chemical approaches for protein stability.

5. References

Abrosimova, K. V., Shulenina, O. V., & Paston, S. V. (2016). FTIR study of the secondary structure of bovine serum albumin and ovalbumin. *Journal of Physics: Conference Series*,769,01,2016.https://doi.org/10.1088/1742-6596/769/1/012016

Ballauff, M. (2022). Denaturation of proteins: electrostatic effects *vs.* hydration. *RSC Advances*, *12*(16), 10105–10113. https://doi.org/10.1039/d2ra01167k

Baronio, C. M., & Barth, A. (2020). The amide I spectrum of proteins—optimization of transition dipole coupling parameters using density functional theory calculations. *The Journal of Physical Chemistry B*, *124*(9), 1703–1714. https://doi.org/10.1021/acs.jpcb.9b11793

Bier, J. M., Verbeek, C. J. R., & Lay, M. C. (2014). Thermal Transitions and Structural Relaxations in Protein-Based Thermoplastics. *Macromolecular Materials and Engineering*, *299*(5), 524–539. https://doi.org/10.1002/mame.201300248

Burbidge, A. S., & le Révérend, B. J. D. (2016). Biophysics of food perception. *Journal of*

Physics D: Applied Physics, *49*(11), 114001. https://doi.org/10.1088/0022-3727/49/11/114001

Clark, T., Heske, J., & Kühne, T. D. (2019). Opposing electronic and nuclear quantum effects on hydrogen bonds in H_2O and D_2O. *ChemPhysChem*, *20*(19), 2461.

Coimbra, J. S. D. R., Gabas, A. L., Minim, L. A., Rojas, E. E. G., Telis, V. R. N., & Telis-Romero, J. (2006). Density, heat capacity and thermal conductivity of liquid egg products. *Journal of Food Engineering*, *74*(2),186–190. https://doi.org/10.1016/j.jfoodeng.2005.01.043

Ferreira, M., Hofer, C., & Raemy, A. (1997). A calorimetric study of egg white proteins. *Journal of Thermal Analysis*, *48*(3), 683–690. https://doi.org/10.1007/bf01979514

Fulczyk, A., Łata, E., Talik, E., Kowalska, T., & Sajewicz, M. (2019). Impact of D2O on the peptidization of l-methionine. *Reaction Kinetics, Mechanisms and Catalysis*, *126*(2), 939–949. https://doi.org/10.1007/s11144-019-01538-4

Goldenzweig, A., & Fleishman, S. J. (2018). Principles of protein stability and their application in computational design. *Annual Review of Biochemistry*, *87*(1), 105–129. https://doi.org/10.1146/annurev-biochem-062917-012102

Hu, C., & Xie, J. (2021). The Effect of Multiple Freeze–Thaw Cycles on the Microstructure and Quality of Trachurus murphyi. *Foods*, *10*(6), 1350. https://doi.org/10.3390/foods10061350

Hu, L., Ying, Y., Zhang, H., Liu, J., Chen, X., Shen, N., Li, Y., & Hu, Y. (2021). Advantages of liquid nitrogen freezing in long-term frozen preservation of hairtail (*Trichiurus haumela*): Enzyme activity, protein structure, and tissue structure. *Journal of Food Process Engineering*, *44*(9),e13789. https://doi.org/10.1111/jfpe.13789

Jackson, M., & Mantsch, H. H. (1995). The use and misuse of FTIR spectroscopy in the determination of protein structure. *Critical reviews in biochemistry and molecular biology*,*30*(2),95–120. https://doi.org/10.3109/10409239509085140

Kocetkovs, V., Radenkovs, V., Juhnevica-Radenkova, K., & Muizniece-Brasava, S. (2022). Variation in the Fatty Acid and Amino Acid Profiles of Pasteurized Liquid Whole Hen Egg Products Stored in Four Types of Packaging. *Animals: an open access journal from MDPI*, *12*(21), 2990. https://doi.org/10.3390/ani12212990

Kong, J., & Yu, S. (2007). Fourier transform infrared spectroscopic analysis of protein secondary structures. *Acta Biochimica et Biophysica Sinica*, *39*(8), 549–559. https://doi.org/10.1111/j.1745-7270.2007.00320.x

Lee, C. K., Yi, B. R., Kim, S. H., Choi, H. S., Kim, M. J., & Lee, J. H. (2018). Volatile profiles and involvement step of moisture in bulk oils during oxidation by action of deuterium oxide (D_2O). *Food science and biotechnology*, *27*(5), 1327–1332. https://doi.org/10.1007/s10068-018-0380-7

Lee, C., Cheon, G. W., Kim, D. H., & Kang, J. U. (2016). Feasibility study: protein denaturation and coagulation monitoring with speckle variance optical coherence tomography. *Journal of Biomedical Optics*, *21*(12),125004. https://doi.org/10.1117/1.jbo.21.12.125004

Lee, S., Jo, K., Jeong, H. G., Choi, Y. S., Kyoung, H., & Jung, S. (2022). Freezing-induced denaturation of myofibrillar proteins in frozen meat. *Critical Reviews in Food Science and Nutrition*, 1–18. 1–18. Advance online publication. https://doi.org/10.1080/10408398.2022.2116557

Li, F., Dong, J., Ren, Y., Kong, B., Wang, B., Xia, X., & Bao, Y. (2021). Impact of ice structuring protein on myofibrillar protein aggregation behaviour and structural property of quick-frozen patty during frozen storage. *International Journal of Biological Macromolecules*, *178*, 136–142. https://doi.org/10.1016/j.ijbiomac.2021.02.158

Liu, L. L., Wang, H., Ren, G. Y., Duan, X., Li, D., & Yin, G. J. (2015). Effects of freeze-drying and spray drying processes on functional properties of phosphorylation of egg white protein. *International Journal of Agricultural and Biological Engineering, 8*(4), 116-123.

Luo, X., Wang, Q., Wu, Y., Duan, W., Zhang, Y., Geng, F., Song, H., Huang, Q., & An, F. (2022). Mechanism of effect of heating temperature on functional characteristics of thick egg white. *LWT*, *154*, 112807. https://doi.org/10.1016/j.lwt.2021.112807

Mettler Toledo. (2022, August 12). *Application Handbooks from the technology leader in thermal analysis*. Mettler Toledo. Retrieved October 18, 2022, from http://www.mt.com/ta-handbooks

Ogawa, N., Mineki, M., Nakamura, Y., Shimoyamada, M., & Watanabe, K. (2003). Rheological and microstructural characteristics of heat-induced gels of egg white proteins and ovalbumin dry-heated at 120°C. *Journal of Cookery Science of Japan*, *36,* 210-218.

Oh, S., Lee, C., Kim, S., Choi, H., Kim, M. J., & Lee, J. (2017). Oxidative Stability and Volatile Formations in Linoleic Acid-D2O Models in the Presence of Deuteron or Electron Donors. *Journal of the American Oil Chemists' Society*, *94*(11), 1385–1392. https://doi.org/10.1007/s11746-017-3044-5

Oshima, H., Yoshidome, T., Amano, K., & Kinoshita, M. (2009). A theoretical analysis on characteristics of protein structures induced by cold denaturation. *Journal of Chemical Physics*, *131*(20), 205102. https://doi.org/10.1063/1.3265985

Pica, A., & Graziano, G. (2017). Effect of heavy water on the conformational stability of globular proteins. *Biopolymers*, *109*(10), e23076. https://doi.org/10.1002/bip.23076

Preethi, R., Shweta, D. S., Moses, J. A., & Anandharamakrishnan, C. (2021). Conductive hydro drying as an alternative method for egg white powder production. *Drying Technology*, *39*(3), 324–336. https://doi.org/10.1080/07373937.2020.1788073

Privalov, P. L. (1990). Cold Denaturation of Protein. *Critical Reviews in Biochemistry and Molecular Biology*, *25*(4), 281–306. https://doi.org/10.3109/10409239009090612

Rossi, M., & Schiraldi, A. (1992). Thermal denaturation and aggregation of Egg Proteins. *Thermochimica Acta*, *199*, 115–123. https://doi.org/10.1016/0040-6031(92)80255-u

Sanfelice, D., & Temussi, P. A. (2016). Cold denaturation as a tool to measure protein stability. *Biophysical Chemistry*, *208*, 4–8. https://doi.org/10.1016/j.bpc.2015.05.007

Schnauß, J., Kunschmann, T., Grosser, S., Mollenkopf, P., Zech, T., Freitag, J. S., Prascevic, D., Stange, R., Röttger, L. S., Rönicke, S., Smith, D. M., Bayerl, T. M., & Käs, J. A. (2021). Cells in slow motion: Apparent undercooling increases glassy behavior at physiological temperatures. *Advanced Materials*, *33*(29), 2101840. https://doi.org/10.1002/adma.202101840

Sen, A., Balamurugan, V., Rajak, K. K., Chakravarti, S., Bhanuprakash, V., & Singh, R. K. (2009). Role of heavy water in biological sciences with an emphasis on thermostabilization of vaccines. *Expert Review of Vaccines*, *8*(11), 1587–1602. https://doi.org/10.1586/erv.09.105

Sun, Z., Yang, F., Li, X., Zhang, C., & Xie, X. (2016). [Effects of Freezing and Thawing Treatments on Beef Protein Secondary Structure Analyzed with ATR-FTIR]. *Spectroscopy and Spectral Analysis*, *36*(11), 3542–3546.

Van Der Plancken, I., Van Loey, A., & Hendrickx, M. (2006). Effect of heat-treatment on the physico-chemical properties of egg white proteins: A kinetic study. *Journal of Food Engineering*, *75*(3), 316–326. https://doi.org/10.1016/j.jfoodeng.2005.04.019

Weiss, I. M., Muth, C., Drumm, R., & Kirchner, H. O. K. (2018). Thermal decomposition of the amino acids glycine, cysteine, aspartic acid, asparagine, glutamic acid, glutamine, arginine and histidine. *BMC Biophysics*, *11*, 2. https://doi.org/10.1186/s13628-018-0042-4

Wootton, M., Hong, N.T., & Thi, H.L. (1981). A Study of the Denaturation of Egg White Proteins during Freezing Using Differential Scanning Calorimetry. *Journal of Food Science*, 46, 1336–1338.

Yousefi, N., & Abbasi, S. (2022). Food proteins: Solubility & thermal stability improvement techniques. *Food Chemistry, 1*, 100090. https://doi.org/10.1016/j.focha.2022.100090

Zhang, Q., Wu, K., Qian, H., Ramachandran, B., & Jiang, F. (2021). The advances of characterization and evaluation methods for the compatibility and assembly structure stability of food soft matter. *Trends in Food Science & Technology*, *112*, 753–763. https://doi.org/10.1016/j.tifs.2021.04.034

Zhao, J.-H., Liu, L.-S., Sablani, S. S., Peng, Y.-J., Xiao, H.-W., Bai, J., & Guo, H. (2020). Comparison of the thermal transitions of spray-dried and freeze-dried egg whites by differential scanning calorimetry. *Food and Bioprocess Technology*, *13*(8), 1329–1343. https://doi.org/10.1007/s11947-020-02477-y

Acknowledgment

We gratefully acknowledge Mr. Markus Bittrich for supporting FT-IR and thermal analyses.

Conflict of Interest

None to declare.

Authors' Contribution

İ.H. Tekiner conceptualized the study, did the project administration, and wrote the original draft of the paper. A. Knoblauch, A. Sover, P. Häfner and N. Muschler performed the investigation and executed the experiments. M. Tainsa edited the final draft of the paper and did the visualization.